Muon lateral distribution function of extensive air showers: Results of the Sydney University Giant Air-shower Recorder versus modern Monte Carlo simulations

N. N. Kalmykov,[1] I. S. Karpikov,[2,*] G. I. Rubtsov,[2] and S. V. Troitsky[2]

[1]*D. V. Skobeltsyn Institute of Nuclear Physics, M. V. Lomonosov Moscow State University, Moscow 119991, Russia*

[2]*Institute for Nuclear Research of the Russian Academy of Sciences, 60th October Anniversary Prospect 7a, Moscow 117312, Russia*

(Received 6 February 2022; accepted 5 April 2022; published 4 May 2022)

The Sydney University Giant Air-shower Recorder (SUGAR) measured the muon component of extensive air showers with a unique array of muon detectors. The SUGAR data allow us to reconstruct the empirical dependence of muon density on the distance from the axis of the shower, the lateral distribution function. We compare the shape of this function with the predictions of hadronic-interaction models, QGSJET-II-04 and EPOS-LHC, in the energy range $10^{17.6}$–$10^{18.6}$ eV. We find a difference between the observed data and the simulation: the observed muon density falls faster with the increased core distance than is predicted in simulations. This observation may be important for interpretation of the energy-dependent discrepancies in the simulated and observed numbers of muons in air showers, known as the "muon excess."

DOI: 10.1103/PhysRevD.105.103004

I. INTRODUCTION

Ultra-high-energy cosmic rays (UHECRs) enable particle-physics studies beyond the capabilities of terrestrial colliders. However, due to their low flux, UHECRs can only be observed indirectly, via extensive air showers (EASs). Hadronic interactions play an important role in the EAS development. Modeling of the hadronic component of EASs is important for studying the primary composition of cosmic rays [1]. The number of muons in EASs is directly related to the hadronic interactions. Recently, much attention has been paid to the discrepancies between the number of muons in theoretical models of the development of EAS, implemented in Monte Carlo simulations, and in real EAS data; see, e.g., Refs. [2,3] for reviews. Some experiments reported this "muon excess" at various primary energies, muon energies, zenith angles, atmospheric depths, and core distances (SUGAR [4–6], HiRes-MIA [7], NEVOD-DECOR [8,9], Yakutsk [10], Pierre Auger Observatory and AMIGA [11,12], and Telescope Array [13]). However, other measurements, performed under different conditions, show the agreement in the muon number between data and models (EAS-MSU [14], Yakutsk [15], KASCADE-Grande [16], and IceTop [17]).

Reference [2] presented a joint analysis of the EAS muon content measured by various experiments (EAS-MSU, IceTop, KASCADE-Grande, NEVOD-DECOR, Pierre Auger Observatory, AMIGA, SUGAR, Telescope Array, and Yakutsk). It has been shown that, on average, the difference between the observed and predicted muon densities grows with the primary energy. However, higher-energy events are rare and are recorded by larger installations; hence, often the muon content of higher-energy EAS is measured at larger distances from the core than for lower energies. Therefore, the change of the shape of the muon lateral distribution function (LDF) and the energy dependence of its normalization may become degenerate. To study the muon LDF, an installation with a large array of muon detectors is best suited.

In this work, we use the data of the Sydney University Giant Air-shower Recorder (SUGAR) (see, e.g., Refs. [18–20]). The main SUGAR dataset is based on observation of muons with shielded detectors only. However, surface-located spark chambers were used to study the electromagnetic component as well, and their results were probably the first demonstration of the muon excess in air showers [4,5]. In a previous work [6], we compared the cosmic-ray spectra measured by SUGAR [21] and by the Pierre Auger Observatory [22,23] and determined the empirical dependence of the number of muons in a vertical shower on the primary energy. This empirical relationship between primary energy and the number of muons was compared with that predicted from the hadronic models, and it was found that the models predicted fewer muons. The purpose of the present work is

*Corresponding author.
karpikov@inr.ru

to determine the experimental muon LDF using the SUGAR data and to compare it with the predictions of Monte Carlo simulations.

The rest of the paper is organized as follows. In Sec. II, we discuss briefly the SUGAR array and the data used, including criteria of event selection. Monte Carlo simulations are described in Sec. III. Section IV describes the procedure of the LDF comparison between data and Monte Carlo simulations and presents our results. We discuss systematic uncertainties of the method in Sec. V and briefly conclude in Sec. VI. Appendixes A and B summarize technical information from previous publications, while Appendix C presents an update of the results of Ref. [6] with a more detailed Monte Carlo simulation performed for the present work and with a revised zenith angle range.

II. SUGAR ARRAY AND ITS DATA

The SUGAR experiment was in operation between 1968 and 1979 [18–20] in New South Wales, Australia, at the altitude of ~250 m above sea level. The array covered an area of about 70 km^2 and consisted of 54 autonomous stations, each consisting of two underground detectors spaced 50 m apart in the North-South direction. Each detector was an underground tank containing a pool of liquid scintillator with an effective area of 6.0 m^2. The detector tanks were buried at the depth of 1.5 m [19]. These detectors, therefore, were intended to record only muons with energies above the threshold of 0.75 $\sec\theta_\mu$ GeV, where θ_μ is the zenith angle of the incident muon. However, each detector station had a maintenance hole on top of it, through which the muon signal was contaminated by the electromagnetic component of a shower for small zenith angles. It has been shown that this contamination is negligible for showers with zenith angles $\theta > 17°$ [24], and in what follows, we include only such events in the analysis. The minimum measured density in the detector was 2.4 vertical equivalent muons per its area of 6 m^2. Each station was triggered and recorded a "local event" when the density in both detectors exceeded 2.4 vertical equivalent muons. The records from the stations were compared with records from all other stations, and the presence of an air shower event was registered when three or more stations could be triggered by the passage of an air shower front through the array. There were 13,729 such events during the 11 years of operation of the array.

For this work, we use the detailed data on these events, which include readings of individual detector stations. The following selection criteria, similar to the standard SUGAR analysis [18–20], were imposed:

(1) The shower axis is located in a square constrained with $|X|$ and $|Y| < 5000$ m.
(2) Events in which the triggered detector is located at a distance from the shower axis of more than 5000 m are removed.
(3) Events with saturated detector stations, > 4000 particles, are removed.
(4) Reconstructed zenith angles are in the range $17° < \theta \leq 70°$.

For each of the events, we determine the effective number of "vertical muons," N_v, using the standard SUGAR procedure; see Appendix A. Then, we make use of the result of Ref. [6], which determined a relation between N_v and the reconstructed primary energy, E, from the normalization to the Auger spectrum (see Appendix B for details). For the present study, we select events with $10^{17.6} < E < 10^{18.5}$ eV (this is the only place where the determination of E is used). The lower energy limit is due to the fact that at $E < 10^{17.6}$ eV the event registration efficiency becomes less than 50%. The upper energy limit is determined by the low statistics of high-energy events. With these selection criteria, $N_{\text{data}} = 4514$ events remain, and we use them to analyze muon LDF.

III. MONTE CARLO SIMULATION

We use the CORSIKA7.4001 [25] EAS simulation package. We choose the QGSJET-II-04 [26] or EPOS-LHC [27] as the high-energy hadronic interaction models and FLUKA2011.2c [28] as the low-energy hadronic interaction model. For each of the two high-energy hadronic interaction models, we simulated 15,000 showers for primary protons and the same number of showers for primary iron, with thrown primary energies following an $E^{-3.19}$ differential spectrum [21] with 9×10^{16} eV $< E < 4 \times 10^{18}$ eV and with zenith angles in the range between 17° and 70°, assuming an isotropic distribution of arrival directions in the celestial sphere. The simulations were performed with the thinning parameter $\epsilon = 10^{-5}$ with the limitation of the maximum weights according to Ref. [29].

While Monte Carlo models of modern experiments include detailed simulations of the detector response to the EAS particles, we find this inappropriate for the present analysis because the available information about the detector and electronics is insufficient for construction of a reliable response model. Instead, we use a traditional approach, where we calculate the expected number of muons at each detector of a station and determine the triggered status of that station by assuming Poisson fluctuations.

For each simulated EAS, we select muons with energies above the detector threshold and calculate their mean numbers in concentric rings around the shower axis, the range 100 m $\leq r \leq$ 1000 m from the axis in ten bins with widths equal in terms of $\log(r)$. These mean densities are used as Poisson means to produce ten readings at artificial "stations," one in each ring. Stations with readings below the threshold of 2.4 vertical equivalent muons were discarded. In addition, we have discarded a certain number of stations to reproduce the distribution of detectors in r

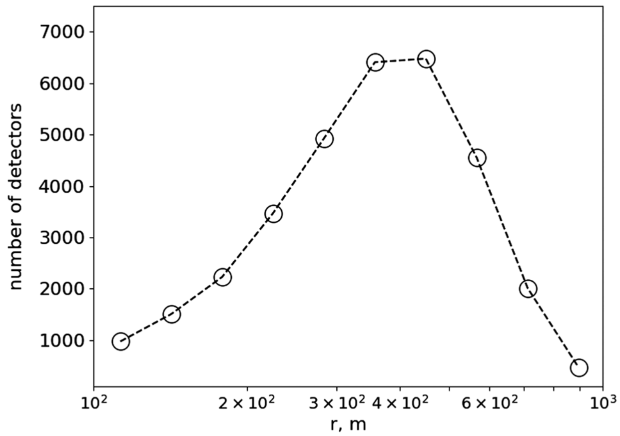

FIG. 1. Distribution of triggered detector stations vs distance from the shower axis. Each point gives the total number of triggered stations of the 4514 selected events in the core-distance bin.

observed in real data; see Fig. 1. The ensemble of these artificial events was treated in the same way as the real data were treated.

IV. ANALYSIS AND RESULTS

In this work, we concentrate on the LDF shape and not on its normalization. Hence, for each event, either real or artificial, we normalize all measured muon densities to the effective total number of muons, N_μ, determined with the standard SUGAR procedure; see Appendix A (note that this normalization is the only step in the analysis where we use the LDF expression adopted by SUGAR). The muon density is multiplied by the normalization factor $10^{6.6}/N_\mu$. We then consider ensembles of real and simulated normalized individual station readings and no longer use the information about EAS events to which these readings were associated. The normalized readings are binned in the core distances in the same ten bins we introduced for the Monte Carlo showers. Then, we compare these normalized binned LDF in the data with the MC (Monte Carlo). The accuracy in determining N_μ in Monte Carlo is $\log_{10}(\Delta N_\mu) = 0.18$.

Figure 2 presents this comparison. We see that the overall agreement between data and simulations is reasonable. Note that at large r the quantities compared and presented in Fig. 2 do not represent the true LDF because we did not account for subthreshold detector stations: the data do not contain information on whether the particular station was in operation at the EAS arrival moment. Zero detector readings were consistently ignored in both data and in MC. This explains the behavior of the function at large r.

To estimate quantitatively the agreement between the data and simulations, we calculate the χ^2 value,

$$\chi^2 = \sum_{i=1}^{\text{bins}} \frac{N_{\text{data}}(P_i^{\text{data}} - P_i^{\text{mc}})^2}{P_i^{\text{data}}}, \qquad (1)$$

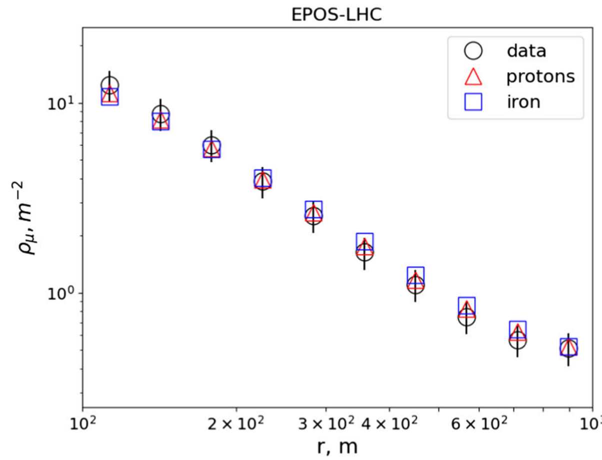

(a)

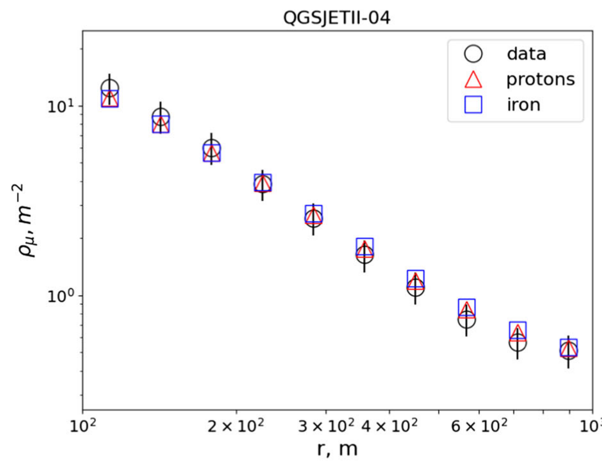

(b)

FIG. 2. Mean muon LDF. Black open circles with error bars indicate the muon LDF of data; red open triangles indicate muon LDF of proton Monte Carlo; blue open squares indicate muon LDF of iron Monte Carlo. Figure 2(a) shows the Monte Carlo simulations with EPOS-LHC; Fig. 2(b) shows Monte Carlo simulations with QGSJET-II-04.

where P_i^{data} and P_i^{mc} are the bin value of the LDF function normalized to 1 (cf. Fig. 2) and $N_{\text{data}} = 4514$ is the total number of events involved in the analysis. For EPOS-LHC, $\chi^2/\text{d.o.f.} = 1.9$ and 3.8 for proton and iron, respectively; for QGSJET-II-04, $\chi^2/\text{d.o.f.} = 2.3$ and 3.5 for proton and iron, respectively.

We observe some difference between the experimental data and Monte Carlo: at close distances, the muon density in the data is higher than in Monte Carlo, and at large distances, on the contrary, the muon density in the data is less than in Monte Carlo. The ratio of the observed and simulated LDF demonstrates this clear trend, better seen in Fig. 3. The simulations underestimate the LDF slope: more muons are concentrated at $r \lesssim 200$ m in the data than is predicted by models. This effect is statistically significant, with the probability to be caused by chance $p \approx 0.007$,

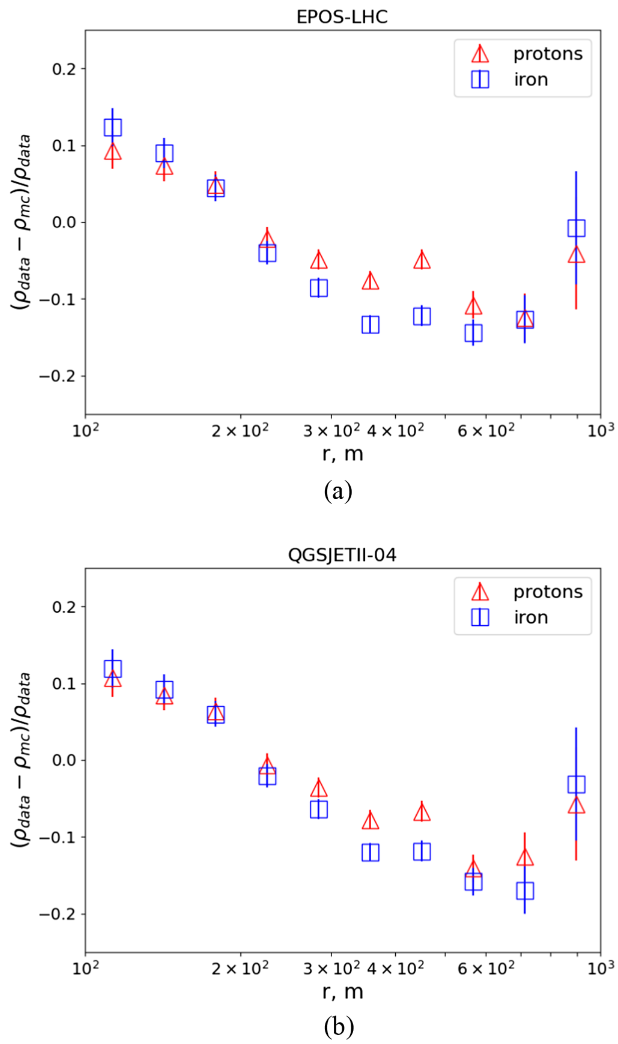

FIG. 3. Fractional difference between the experimental and simulated muon LDF. Red open triangles indicate muon LDF of proton Monte Carlo; blue open squares indicate muon LDF of iron Monte Carlo. Error bars correspond to statistical uncertainly. Figure 3(a): the Monte Carlo simulations with EPOS-LHC; Fig. 3(b): the Monte Carlo simulations with QGSJET-II-04.

estimated by the Pearson's chi-squared method. This trend is present for both hadronic-interaction models and both primary particle types we considered.

V. SYSTEMATIC UNCERTAINTIES

In the present study, we concentrate only on the shape of the LDF, which reduces considerably systematic uncertainties, compared to studies of the LDF normalization, the muon excess. Let us discuss briefly potential sources of systematics.

A. Energy scale

We discuss the energy determination and corresponding uncertainties in Ref. [6] and summarize the discussion in Appendix B. As we have already pointed out, for the present analysis, the primary energy is used only to select the events for the dataset. The uncertainty of the energy scale translates into the uncertainty of the range of energies to which our results are applicable but does not affect the results themselves since we are studying the shape of the normalized LDF. The change of the energy scale might manifest itself only if the shape of the muon LDF depended strongly on the primary energy within the energy range of interest. We tested that this is not so by repeating our analysis for two parts of the dataset, with primary energies $10^{17.6}$ eV $\leq E < 10^{18.0}$ eV and $10^{18.0}$ eV $\leq E \leq 10^{18.5}$ eV. The difference in the LDF shape between the two subsets is negligible and does not exceed 0.01 in terms of the fractional difference plotted in Fig. 3.

B. Detector calibration

Possible systematic errors in the measurements of the muon density may be related to the absolute detector calibration. However, in the present study, we operate with the normalized LDF; since the errors of this class affect the overall LDF scale, they cancel at normalization.

C. Nonlinearity

However, in case there exist certain nonlinearity related to the saturation effects, it may affect the LDF shape because the saturated detectors are always located at small core distances. We cannot find a detailed description of the nonlinearity in SUGAR detectors, and therefore in our analysis, we excluded all events for which at least one detector was saturated; see Sec. II. To test the potential effect of nonlinearities, we lowered the saturation threshold by a factor of 2 and repeated our analysis. The change in the results was negligible compared to the statistical errors.

VI. CONCLUSIONS

We have used the data on muon content of EASs caused by primary cosmic-ray particles with energies $\sim 10^{18}$ eV and recorded by SUGAR to study the shape of the muon LDF and to compare it with the predictions of hadronic-interaction models EPOS-LHC and QGSJET-II-04. We found that both models predict a slower decrease of the muon density with increasing core distance for both proton and iron primaries than is observed in the data; see Fig. 3. We also used improved Monte Carlo simulations performed for this work to update our previous results on the muon content of SUGAR-detected EASs reported in Ref. [6]; see Appendix C.

ACKNOWLEDGMENTS

We are indebted to Juris Ulrichs for his help and support crucial for our work with the SUGAR data and for intense discussions of the analysis. The results of this paper have been presented and discussed in the Working Group on Hadronic Interactions and Shower Physics, to participants of which we are indebted for interesting comments. We thank Leonid Bezrukov for helpful discussions and the anonymous reviewer for careful reading of the manuscript and numerous helpful comments. Monte Carlo simulations have been performed at the computer cluster of the Theoretical Physics Department, Institute for Nuclear Research of the Russian Academy of Sciences. Development of the analysis methods (I. K. and G. R.) was supported by the Russian Science Foundation (Grant No. 17-72-20291).

APPENDIX A: NORMALIZATION

The muon number, N_μ, is determined by fitting individual detector readings by the experimentally determined muon LDF [4,5],

$$\rho_\mu(r) = N_\mu k(\theta)\left(\frac{r}{r_0}\right)^{-a}\left(1+\frac{r}{r_0}\right)^{-b}. \qquad \text{(A1)}$$

Here, ρ_μ is the muon density, N_μ is the estimated total number of muons, θ is the incident zenith angle, r is the perpendicular distance from the shower axis, $r_0 = 320$ m, $a = 0.75$, $b = 1.50 + 1.86\cos\theta$, and

$$k(\theta) = \frac{1}{2\pi r_0^2}\frac{\Gamma(b)}{\Gamma(2-a)\Gamma(a+b-2)}. \qquad \text{(A2)}$$

APPENDIX B: ENERGY ESTIMATION

For a given EAS zenith angle θ, the effective vertical muon number N_v in a shower is related to the reconstructed muon number N_μ through the relation [30]

$$\log_{10}\left(\frac{N_\mathrm{v}}{N_\mathrm{r}}\right) = (1-\gamma_\mathrm{v})^{-1}\cdot(1-\gamma_\mathrm{v}-A(\cos\theta-1)) \times \log_{10}\left(\frac{N_\mu}{N_\mathrm{r}}\right) + B(\cos\theta-1) + \log_{10}\left(\frac{1-\gamma_\mathrm{v}}{1-\gamma_\mathrm{v}-A(\cos\theta-1)}\right), \qquad \text{(B1)}$$

where the coefficients are $A = 0.47$, $B = 2.33$, $\gamma_\mathrm{v} = 3.35$, and the normalization scale is $N_\mathrm{r} = 3.16\times10^7$.

The primary energy of a shower is related to N_v by the expression

$$E = E_\mathrm{r}(N_\mathrm{v}/N_\mathrm{r1})^\alpha, \qquad \text{(B2)}$$

where $N_\mathrm{r1} = 10^7$ and parameters $\alpha = 1.018 \pm 0.0042_\mathrm{stat} \pm 0.0043_\mathrm{syst\ SUGAR} \pm 0.0028_\mathrm{syst\ Auger}$, and $E_\mathrm{r} = (8.67 \pm 0.21_\mathrm{stat} \pm 0.26_\mathrm{syst\ SUGAR} \pm 1.21_\mathrm{syst\ Auger})\times10^{17}$ eV are obtained in Ref. [6] from the comparison of the SUGAR and Auger spectra. Parameters α and E_r were determined [6] from the requirement that the SUGAR spectrum matches the spectrum observed by Auger, which is justified since both experiments have similar fields of view in the Southern hemisphere. As discussed in Ref. [6], the main systematic uncertainty comes therefore from the systematic error of 14% in the Auger energy scale [22].

APPENDIX C: UPDATE ON THE RESULTS OF REF. [6]

Monte Carlo simulations used in Ref. [6] have been improved and corrected for the present work. The new

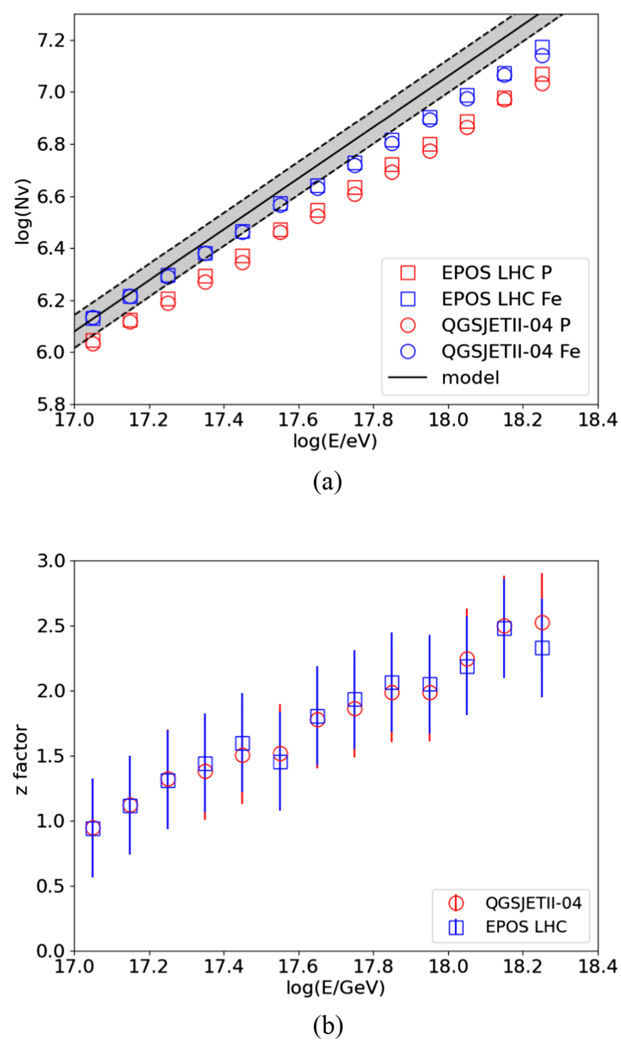

FIG. 4. Update of the results of Ref. [6]. (a) Mean effective number of vertical muons N_v as a function of the primary energy. Points indicate the results of Monte Carlo simulations with QGSJET-II-04 (protons: red open circles; iron: blue open circles), EPOS-LHC (protons: red open quadrature; iron: blue open quadrature). The gray line corresponds to our empirical model (B2); the shaded gray area indicates the total uncertainly (statistical and systematic errors, see the text, summed in quadrature). (b) The z factor vs the primary energy.

simulations differ in the account of the threshold of the detector signal and the fluctuation of the muon density. In addition, Ref. [6] used all zenith angles $\theta \leq 70°$, which might introduce a bias for near-vertical showers because of the detector maintenance hole discussed above. Here, we present an update of Ref. [6] with the new simulations and for $17° \leq \theta \leq 70°$. In brief, we use the experimental muon LDF (A1) and fit it to the distribution of the muon density in the MC, obtaining N_μ. Then, we use Eq. (B1) to express the effective number of vertical muons N_v in terms of N_μ and θ. As a result, N_v is determined for each shower (both in data and in simulations). Thus, we can plot the dependence of the number of vertical muons on the primary energy and compare it with Eq. (B2) obtained [6] from comparison of the SUGAR and Auger spectra.

To compare the experimental muon density with the simulation predictions, we use the z factor [2],

$$z = \frac{\log_{10}(N_\mathrm{v}^\mathrm{SUGAR}) - \log_{10}(N_\mathrm{v}^\mathrm{p})}{\log_{10}(N_\mathrm{v}^\mathrm{Fe}) - \log_{10}(N_\mathrm{v}^\mathrm{p})}, \tag{C1}$$

where $N_\mathrm{v}^\mathrm{SUGAR}$ is the number of vertical muons calculated by the formula (B2) and N_v^p and N_v^Fe are the simulated mean numbers of vertical muons for proton and iron primaries.

Figure 4(a) presents a comparison of the new simulation results for $N_\mathrm{v}(E)$ with our empirical model (B2). Figure 4(b) shows the dependence of the z factor on energy. Compared with our previous work, the z factor is smaller, so the disagreement in the total muon number between the data and simulations, the muon excess, is more modest. The most probable physical reason for this difference is the contamination of the muon signal by the electromagnetic component for vertical showers, which we did not take into account in Ref. [6]. Since SUGAR measured only muons, potential shifts of the energy scale are degenerate with the shifts in muon number; this systematic uncertainty is dominated by the uncertainty of the Auger energy scale (see Appendix B). Note that this uncertainty does not affect the results of the present work, which studies the shape, and not the normalization, of the LDF; see Sec. V.

[1] K.-H. Kampert and M. Unger, Measurements of the cosmic ray composition with air shower experiments, Astropart. Phys. **35**, 660 (2012).

[2] H. P. Dembinski *et al.* (EAS-MSU, IceCube, KASCADE-Grande, NEVOD-DECOR, Pierre Auger, SUGAR, Telescope Array, Yakutsk EAS Array Collaborations), Report on tests and measurements of hadronic interaction properties with air showers, EPJ Web Conf. **210**, 02004 (2019).

[3] J. Albrecht, L. Cazon, H. Dembinski, A. Fedynitch, K.-H. Kampert, T. Pierog, W. Rhode, D. Soldin, B. Spaan, R. Ulrich, and M. Unger, The muon puzzle in cosmic-ray induced air showers and its connection to the large hadron collider, Astrophys. Space Sci. **367** (2022).

[4] C. J. Bell *et al.*, The structure functions of very large E. A. S., in *International Cosmic Ray Conference*, International Cosmic Ray Conference (University of Denver, Colorado Associated University Press, Boulder, 1973), Vol. 4, p. 2569.

[5] C. J. Bell *et al.*, Structure function of large air showers, in *International Cosmic Ray Conference*, International Cosmic Ray Conference (Max-Planck-Institut für Extraterrestrische Physik, Garching, 1975), Vol. 8, p. 2762.

[6] J. A. Bellido, R. W. Clay, N. N. Kalmykov, I. S. Karpikov, G. I. Rubtsov, S. V. Troitsky, and J. Ulrichs, Muon content of extensive air showers: Comparison of the energy spectra obtained by the Sydney University Giant Air-shower Recorder and by the Pierre Auger Observatory, Phys. Rev. D **98**, 023014 (2018).

[7] T. Abu-Zayyad *et al.* (HiRes, MIA Collaborations), Evidence for Changing of Cosmic Ray Composition between 10^{17}-eV and 10^{18}-eV from Multicomponent Measurements, Phys. Rev. Lett. **84**, 4276 (2000).

[8] A. G. Bogdanov, D. M. Gromushkin, R. P. Kokoulin, G. Mannocchi, A. A. Petrukhin, O. Saavedra, G. Trinchero, D. V. Chernov, V. V. Shutenko, and I. I. Yashin, Investigation of the properties of the flux and interaction of ultrahigh-energy cosmic rays by the method of local-muon-density spectra, Phys. At. Nucl. **73**, 1852 (2010).

[9] A. G. Bogdanov, R. P. Kokoulin, G. Mannocchi, A. A. Petrukhin, O. Saavedra, V. V. Shutenko, G. Trinchero, and I. I. Yashin, Investigation of very high energy cosmic rays by means of inclined muon bundles, Astropart. Phys. **98**, 13 (2018).

[10] A. V. Glushkov, I. T. Makarov, M. I. Pravdin, I. E. Sleptsov, D. S. Gorbunov, G. I. Rubtsov, and S. V. Troitsky, Muon content of ultrahigh-energy air showers: Yakutsk data versus simulations, JETP Lett. **87**, 190 (2008).

[11] A. Aab *et al.* (Pierre Auger Collaboration), Testing Hadronic Interactions at Ultrahigh Energies with Air Showers Measured by the Pierre Auger Observatory, Phys. Rev. Lett. **117**, 192001 (2016).

[12] S. Müller (Pierre Auger Collaboration), Direct measurement of the muon density in air showers with the Pierre Auger observatory, EPJ Web Conf. **210**, 02013 (2019).

[13] R. U. Abbasi *et al.* (Telescope Array Collaboration), Study of muons from ultrahigh energy cosmic ray air showers measured with the Telescope Array experiment, Phys. Rev. D **98**, 022002 (2018).

[14] Y. A. Fomin, N. N. Kalmykov, I. S. Karpikov, G. V. Kulikov, M. Y. Kuznetsov, G. I. Rubtsov, V. P. Sulakov, and S. V. Troitsky, No muon excess in extensive air showers at 100–500 PeV primary energy: EAS–MSU results, Astropart. Phys. **92**, 1 (2017).

[15] A. V. Glushkov and A. V. Saburov, Mass composition of cosmic rays with energies above 10^{17} eV according to the data from the muon detectors of the Yakutsk EAS array, JETP Lett. **109**, 559 (2019).

[16] W. D. Apel *et al.* (KASCADE-Grande Collaboration), Probing the evolution of the EAS muon content in the atmosphere with KASCADE-Grande, Astropart. Phys. **95**, 25 (2017).

[17] R. Abbasi *et al.*, Density of GeV muons in air showers measured with IceTop, arXiv:2201.12635.

[18] C. B. A. McCusker and M. M. Winn, A new method of recording large cosmic-ray air showers, Nuovo Cimento **28**, 175 (1963).

[19] R. G. Brownlee *et al.*, Design of an array to record air showers of energy up to 10^{21} eV, Can. J. Phys. **46**, S259 (1968).

[20] C. J. Bell *et al.*, The upper end of the observed cosmic ray energy spectrum, J. Phys. A **7**, 990 (1974).

[21] M. M. Winn, J. Ulrichs, L. S. Peak, C. B. A. Mccusker, and L. Horton, The cosmic ray energy spectrum above 10^{17} eV, J. Phys. G **12**, 653 (1986).

[22] A. Aab *et al.* (Pierre Auger Collaboration), The Pierre Auger Cosmic Ray Observatory, Nucl. Instrum. Methods Phys. Res., Sect. A **798**, 172 (2015).

[23] Edited by D. Veberic, *The Pierre Auger Observatory: Contributions to the 35th International Cosmic Ray Conference (ICRC 2017)* (Bexco, Busan, 2017), arXiv:1708.06592.

[24] L. S. Wilson, A study of muons and electrons in large cosmic ray air showers, Ph.D. thesis, University of Sydney, Sydney, NSW, Australia, 1973.

[25] D. Heck, J. Knapp, J. N. Capdevielle, G. Schatz, and T. Thouw, CORSIKA: A Monte Carlo code to simulate extensive air showers, Technical Report, FZKA, 1998.

[26] S. Ostapchenko, Monte Carlo treatment of hadronic interactions in enhanced Pomeron scheme: I. QGSJET-II model, Phys. Rev. D **83**, 014018 (2011).

[27] T. Pierog, I. Karpenko, J. M. Katzy, E. Yatsenko, and K. Werner, epos lhc: Test of collective hadronization with data measured at the CERN Large Hadron Collider, Phys. Rev. C **92**, 034906 (2015).

[28] G. Battistoni, S. Muraro, P. R. Sala, F. Cerutti, A. Ferrari, S. Roesler, A. Fasso, and J. Ranft, The FLUKA code: Description and benchmarking, AIP Conf. Proc. **896**, 31 (2007).

[29] M. Kobal (Pierre Auger Collaboration), A thinning method using weight limitation for air-shower simulations, Astropart. Phys. **15**, 259 (2001).

[30] L. Horton, C. B. A. McCusker, L. S. Peak, J. Ulrichs, and M. M. Winn, Muon-size spectrum of large EAS, in *International Cosmic Ray Conference*, International Cosmic Ray Conference (Tata Institute of Fundamental Research, Colaba, Bombay, 1983), Vol. 6, p. 124.